# Selective catalytic reduction of $NO_x$ by hydrogen over modified $Pd/TiO_2$-$Al_2O_3$ catalyst under lean-burn conditions

Kaijiao Duan · Zhiming Liu · Lei Yuan

**Abstract** A series of Ni, Sn and Ca modified $Pd/TiO_2$-$Al_2O_3$ catalysts were prepared by the incipient wetness impregnation method and their catalytic performance for the selective catalytic reduction of $NO_x$ by $H_2$ was evaluated. The results showed that the $NO_x$ conversion and $N_2$ selectivity were improved over $Pd$-$Sn/TiO_2$-$Al_2O_3$ and $Pd$-$Ni/TiO_2$-$Al_2O_3$ catalysts above 200 °C. More importantly, the $N_2$ selectivity and high-temperature activity of $Pd$-$Sn/TiO_2$-$Al_2O_3$ catalyst was far superior to the single $Pd/TiO_2$-$Al_2O_3$ catalyst. The optimal Sn loading was 2 wt.%. X-ray diffraction (XRD) results showed that the interaction between Pd and Sn promotes the dispersion of Pd over $TiO_2$-$Al_2O_3$. Temperature-programmed reduction ($H_2$-TPR) results demonstrated that the addition of Sn contributes to the formation of $Pd^0$ and improving the redox property of $Pd/TiO_2$-$Al_2O_3$. The additives of Ni and Sn also facilitated the absorption of $NO_x$ and the oxidation of NO to $NO_2$, which play important roles in the selective catalytic reduction of $NO_x$ by hydrogen.

**Keywords** DeNO*x* · $H_2$-SCR · Sn modification · $Pd/TiO_2$-$Al_2O_3$ · Pd dispersion · NO adsorption and oxidation

## 1 Introduction

Nitrogen oxides ($NO_x$) emitted from diesel vehicle are the major air pollutants that greatly contribute to the formation of photochemical smog and acid rain. With the rapid increase of the vehicles, the air pollution in China has become to the combined pollution of coal flue gas and vehicle exhaust [1–3]. Therefore, the removal of $NO_x$ from mobile sources has attracted more and more attention. The conventional three-way catalyst is no longer effective for the removal of $NO_x$ in the presence of oxygen. Selective catalytic reduction (SCR) of $NO_x$ with different reducing agents is an effective method for the control of $NO_x$ under lean-burn conditions.

In the $NH_3$-SCR of $NO_x$, besides the "$NH_3$ slip", the formed ammonium nitrate and ammonium sulfate at low temperatures can occupy the active sites and result in the activity loss of the catalyst [4, 5]. For the HC-SCR, the low-temperature activity of the catalyst needs to be improved to reduce $NO_x$ emitted from diesel vehicle [6, 7]. Recently, $H_2$-SCR has attracted attention because in this process $H_2$ can efficiently reduce $NO_x$ at low temperatures (100 to 300 °C) [8–15]. Another advantage of this technique is that the surplus hydrogen will react with oxygen to form water with zero pollution. The following are the two main reactions occur in the $H_2$-SCR of $NO_x$:

$$2NO + 4H_2 + O_2 \rightarrow N_2 + 4H_2O \tag{1}$$

$$4NO + 4H_2 + O_2 \rightarrow 2N_2O + 4H_2O \tag{2}$$
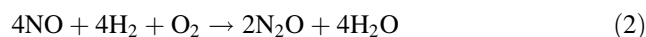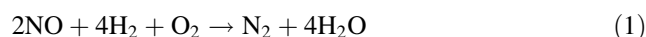
The greenhouse gas $N_2O$ may be formed in the $H_2$-SCR through reaction (2). Therefore, the catalyst which can promote the reaction (1) to proceed while inhibiting the reaction (2) is desirable. Pt and Pd-based catalysts have shown to be active for the $H_2$-SCR of $NO_x$. Since Pd is less costly than Pt, Pd-based catalysts have been paid more and more attention. Improving the $NO_x$ conversion and $N_2$ selectivity are the main targets in the development of Pd-based catalysts for the $H_2$-SCR. Melanie et al. [16] found that the addition of W can promote the $H_2$-deNO*x* activity

---

K. Duan · Z. Liu (✉) · L. Yuan
State Key Laboratory of Chemical Resource Engineering,
Beijing University of Chemical Technology,
Beijing 100029, China
e-mail: liuzm@mail.buct.edu.cn

of Pd/ZrO$_2$ catalyst. Pd was predominately present in the form of PdO with particle sizes smaller than 2 nm due to the addition of W. However, the reaction temperature window of the catalyst was too narrow to meet the demand of vehicle exhaust emission control. Greenhalgh et al. [17] have studied a series of Fe, Co and K modified Pd/Al$_2$O$_3$-TiO$_2$ catalysts for the H$_2$-SCR. They found that the added Co promoted the N$_2$ selectivity at low temperature, while K not only enhanced the N$_2$ selectivity but also increased the activity at high temperatures. Yue et al. [18] reported that Ca showed a promoting effect on the catalytic performance of Pd/Ce-Zr/Al$_2$O$_3$. The addition of Ca to Pd/Ce-Zr/Al$_2$O$_3$ induced the well-dispersion of PdO particles on the support and improved the reduction/reoxidation property and thermal stability of the active PdO species, and thus enhanced the catalytic activity and thermal stability of the Pd/Ce-Zr/Al$_2$O$_3$ catalyst. The promoting effect of Ca on Pd/Ce-Zr/Al$_2$O$_3$ catalyst was also reported by Wang et al. [19]. SnO$_2$ was reported to be active in the HC-SCR of NO$_x$ [20, 21]. Corro et al. [22] found that the addition of Sn to Pt/Al$_2$O$_3$ can prevent Pt particles from sintering at high temperatures, thus leading to the enhanced the activity, N$_2$ selectivity and SO$_2$ resistance above 200 °C in the C$_3$H$_8$-SCR. For Ni a typical transition metal, Li et al. [23] reported that the addition of transition metal Ni to Pd catalyst can lead to higher stability than the Pd alone. Amin et al. [24] found that PdNi alloy was formed with an average particle size of 3 nm over Pd-Ni/C catalyst. Pd-Ni/C showed better stability than Pd/C and Ni/C. These facts indicated that the activity and selectivity of the catalyst can be improved by the added promoter through strengthening the interaction between the different metals and promoting the dispersion of the active sites.

In the present study, a series of Ni, Sn and Ca modified Pd/TiO$_2$-Al$_2$O$_3$ catalysts were prepared by the incipient wetness impregnation method and their catalytic performance for the selective catalytic reduction of NO$_x$ by H$_2$ was evaluated. The results showed that the NO$_x$ conversion and N$_2$ selectivity were improved due to the addition of Ni and Sn above 200 °C. These catalysts were further characterized by N$_2$ adsorption, X-ray diffraction (XRD), temperature-programmed desorption of NO$_x$ (NO$_x$-TPD) and temperature-programmed reduction (H$_2$-TPR). The relationship between the H$_2$-SCR performance and the catalyst structure has been elucidated.

## 2 Experimental

### 2.1 Catalyst preparation

For the preparation of porous Al$_2$O$_3$, 60.9 g aluminum isopropoxide was added in 400 mL deionized water, then the mixture was placed in round bottom flask equipped in rotary evaporator and hydrolyzed in hot water (85 °C) with 3–4 mL nitric acid. After 3 h rotating, the aluminium boehmite gel was obtained by vacuum filtration. Subsequently, the sample was placed at room temperature for 12 h, dried at 120 °C and calcined at 600 °C for 4 h to obtain Al$_2$O$_3$. TiO$_2$-Al$_2$O$_3$ support was prepared by mechanically mixing the obtained Al$_2$O$_3$ and P25 (Degussa AEROSIL TiO$_2$ P25) at the mass ratio of 1:1, and then grinded and stirred at 40 °C for 5 h, the product was finally dried at 120 °C for 12 h.

0.5%Pd-2%Ni/TiO$_2$-Al$_2$O$_3$, 0.5%Pd-$x$%Sn/TiO$_2$-Al$_2$O$_3$ ($x$ = 1, 2, 5) and 0.5%Pd-2%Ca/TiO$_2$-Al$_2$O$_3$ were prepared by the incipient wetness of impregnation method. A 3 g TiO$_2$-Al$_2$O$_3$ was added into the proper amount of Ni(NO$_3$)$_2$·6H$_2$O, SnCl$_4$ and Ca(NO$_3$)$_2$·4H$_2$O solution, respectively, followed by drying at 120 °C for 12 h. Then the samples were incorporated into PdCl$_4$ solution, dried at 120 °C for 12 h and calcined at 500 °C for 4 h. 0.5%Pd/TiO$_2$-Al$_2$O$_3$ was also prepared in the same way described above. Here-in-after 0.5%Pd-2%Ni/TiO$_2$-Al$_2$O$_3$, 0.5%Pd-$x$%Sn/TiO$_2$-Al$_2$O$_3$ ($x$ = 1, 2, 5), 0.5%Pd-2%Ca/TiO$_2$-Al$_2$O$_3$ and 0.5%Pd/TiO$_2$-Al$_2$O$_3$ catalysts are designed by Pd-Ni, Pd-Sn, Pd-Ca and Pd, respectively.

### 2.2 Catalytic test

The evaluation of the H$_2$-SCR performance of the catalyst was carried out in a fixed-bed quartz flow reactor using a 0.2 g catalyst of 40–60 mesh. The feed gas mixture contained 0.25 % NO, 1 % H$_2$ and 5 % O$_2$ in a He balance. The total flow rate of the feed gas was 200 mL min$^{-1}$, corresponding to a space velocity of 40,000 h$^{-1}$. The composition of the product gas was analyzed by gas chromatograph (Shimadzu GC 2014, equipped with Porapak Q and Molecular sieve 5A columns, Japan) and a chemiluminescence NO/NO$_2$ analyzer (42i-HL, Thermal environmental instrument, USA). The reaction temperature was increased from 100 to 400 °C and the activity data were collected when the catalytic reaction practically reached steady-state condition at each temperature. The performances of catalysts were evaluated by means of NO$_x$ conversion and N$_2$ selectivity as described by the following equations:

$$NO_x \text{ conversion} = \frac{C_{NO_x \text{ inlet}} - C_{NO_x \text{ outlet}}}{C_{NO_x \text{ inlet}}} \times 100\,\%, \qquad (3)$$

$$N_2 \text{ selectivity} = \frac{C_{N_2 \text{ outlet}}}{C_{N_2O \text{ outlet}} + C_{N_2 \text{ outlet}}} \times 100\,\%. \qquad (4)$$

### 2.3 Catalyst characterization

Characterization of the Brunauer-Emmett-Teller (BET) surface area of the catalyst was carried out with a

Quantachrome Autosorb AS-1 system (USA) at liquid $N_2$ temperature (–196 °C). The specific surface area, pore volume and pore size distribution of the catalysts were determined by BET and Barrett-Joyner-Halenda (BJH) methods. Powder XRD measurements recorded on a Brucker D8 Advanced system (Germany) with Cu Kα radiation at 45 kV and 200 mA. $NO_x$-TPD was performed on a fixed-bed quartz reactor using 0.2 g catalyst. The concentrations of NO, $NO_2$ and $NO_x$ were detected on a chemiluminescence $NO/NO_2$ analyzer. Before the experiment, the catalyst was pretreated in pure He at 400 °C for 1 h. After the catalyst was cooled down to room temperature in pure He, the He flow was switched into 0.25 % NO and 5 % $O_2$ (balanced with He) for 1 h with the total flow rate of 200 mL min$^{-1}$. After being saturated, the sample was degassed by He to remove the physically adsorbed NO and $NO_2$. The sample was then purged in pure He with the heating rate of 10 °C min$^{-1}$ to 600 °C. Temperature-programmed reduction ($H_2$-TPR) experiments were conducted on a chemisorptions analyzer (Micromeritics, ChemiSorb 2720 TPx, USA) under a 5 % $H_2$ gas flow (100 mL min$^{-1}$) at a rate of 10 °C min$^{-1}$ to 500 °C. Each catalyst was pretreated at 300 °C in helium for 1 h before test.

## 3 Results and discussion

### 3.1 H2-SCR activity

#### 3.1.1 Comparison of the H2-SCR performance

Figure 1 shows the NO conversion (a) and $N_2$ selectivity (b) for the SCR of NO with $H_2$ over Pd, Pd-Ni, Pd-Sn and Pd-Ca catalysts. From Fig. 1a it can be seen that $NO_x$ conversion is improved by the addition of Ni and Sn, and Pd-Sn shows the widest temperature window and the

highest $NO_x$ conversion above 200 °C. On the contrary, $H_2$-SCR activity is decreased over Pd-Ca catalyst. The "volcano-type" behavior of $NO_x$ conversion as a function of temperature is observed in Fig. 1a. On one hand, the combustion reaction of $H_2$ with $O_2$ above 150 °C becomes predominant, leading to less remained reductant for the SCR reaction and thus a drop of $NO_x$ conversion. On the other hand, the partial oxidation of Pd under $H_2$-SCR occurred above 150 °C, the chemical nature change of Pd could lower the surface coverage of hydrogen on its surface, and in turn the rate of H-spillover from Pd to the support interface, and thus the rate of $NO_x$ reduction [14]. Besides the activity, $N_2$ selectivity is also greatly increased over Pd-Sn and Pd-Ni catalysts compared with Pd alone. Obviously, the $N_2$ selectivity on all catalysts gradually decreased with increasing temperature. At low temperature the reaction route is H-assisted dissociation of NO dominating on active sites, while at high temperature the route is accomplished by H-assisted reduction of nitrates on the support. $N_2O$ can be produced by the decomposition of surface nitrate, thus resulting in the decreased $N_2$ selectivity [25, 26]. Despite all that more than 70 % $N_2$ selectivity was obtained in the temperature range of 100–400 °C over Pd-Sn catalyst. Therefore, the additives of Sn and Ni are favorable for improving the activity and selectivity of Pd catalyst for the $H_2$-SCR of $NO_x$, and the promoting effect is more noticeable in the case of Sn modification. Compared to the previously reported Pd-Ir/$TiO_2$ [25] and Pd-$K_2O$/$TiO_2$ catalysts [26], Pd-Sn and Pd-Ni showed much higher $N_2$ selectivity for the $H_2$-SCR of $NO_x$.

#### 3.1.2 Effect of Sn loading on the H2-SCR performance

Since Sn showed a more noticeable promoting effect on Pd catalyst for the $H_2$-SCR of $NO_x$, the effect of Sn loading on the catalytic performance of Pd catalyst for the $H_2$-SCR of
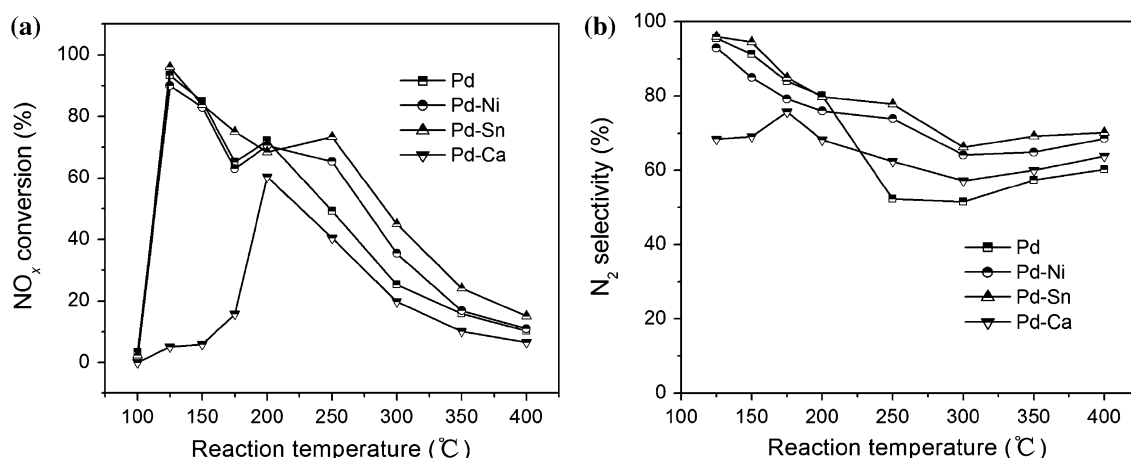


Fig. 1 H2-SCR performance over Ni, Sn and Ca modified Pd and single Pd catalysts. a $NO_x$ conversion; b $N_2$ selectivity

NO$_x$ was further investigated and the results are shown in Fig. 2. From Fig. 2a it can be seen that 1 % Sn additive leads to a slight increase of NO$_x$ conversion. With increasing Sn loading to 2 %, NO$_x$ conversion is significantly improved above 200 °C. The further increase of the Sn loading to 5 % results in the decrease of the NO$_x$ conversion. From Fig. 2b it is evident that the addition of Sn promotes the N$_2$ selectivity and the optimal loading is also 2 %.

## 3.2 BET surface area and XRD

The textural properties of Pd, Pd-Ni, Pd-Sn and Pd-Ca were characterized and the results are summarized in Table 1. It is seen that the addition of Ni and Sn slightly increased the specific surface area. While the added Ca leads to the decreased specific surface area and increased average particle size, indicating that the dispersion of Pd was suppressed due to the addition of Ca, thus leading to the poor performance of H$_2$-SCR of NO$_x$ on Pd-Ca catalysts.

XRD patterns of Pd and modified Pd catalysts are illustrated in Fig. 3. The diffraction peaks ascribed to the anatase TiO$_2$ phase (101), (004) and (200) ($2\theta = 25.3°$, 37.8°, 48.1°) can be observed. The diffraction peaks at $2\theta = 27.5°$, 36.1°, 41.3°, 54.4°, 56.6° are corresponding to (110), (220), (111), (211) and (220) crystalline of rutile TiO$_2$ phase [27, 28]. γ-Al$_2$O$_3$ diffraction peaks are also observed at $2\theta = 36.4°$, 38.3°, 42.8° and 53.8° [29]. From the XRD results it can be seen that there is little change in the crystallinity of TiO$_2$-Al$_2$O$_3$ support after modification. The peaks assigned to Ni, Ca and Pd species are not observed. The absence of Pd could be due to the low loading and the high dispersion of Pd on the surface of TiO$_2$-Al$_2$O$_3$. The weak reflections near $2\theta = 37.1°$, 47.8° and 62.6° are corresponding to tetragonal SnO [30]. It is

well worth to note that the peaks at $2\theta = 54.2°$ and 41.2° appeared, which are assigned to Pd$_3$Sn$_2$ and Pd$_3$Sn alloy [31, 32], indicating that the strong interaction between Pd and Sn exists, which results in the high dispersion of Pd and high catalytic performance of H$_2$-SCR of NO$_x$.

**Table 1** BET surface area, pore volume, pore size and average particle size of different catalysts

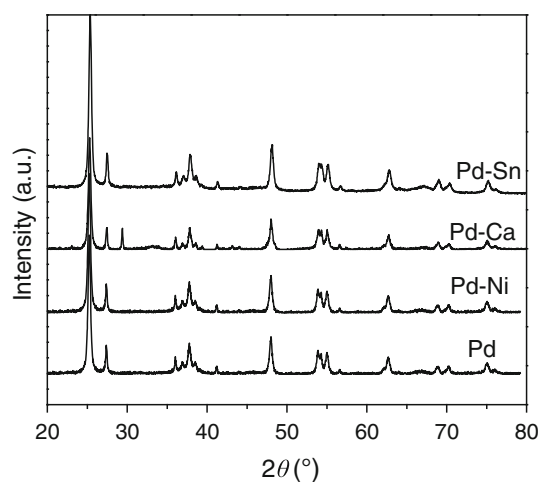| Samples | BET area ($m^2 g^{-1}$) | Pore volume ($cm^3 g^{-1}$) | Pore size (nm) | Average particle size (nm) |
|---------|---------|---------|---------|---------|
| Pd | 132 | 0.48 | 10.9 | 46 |
| Pd-Ni | 134 | 0.38 | 11.4 | 46 |
| Pd-Sn | 133 | 0.32 | 10.1 | 45 |
| Pd-Ca | 125 | 0.36 | 10.5 | 48 |



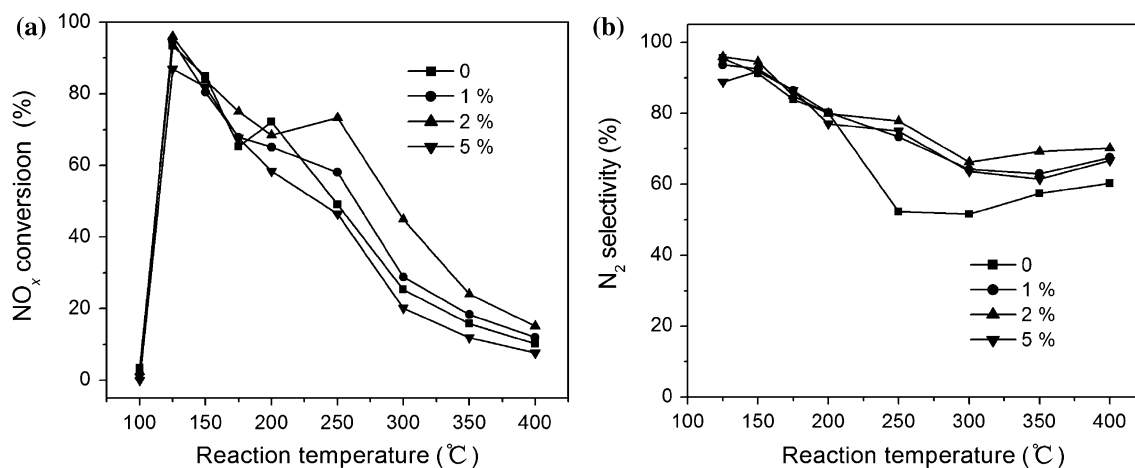**Fig. 3** XRD patterns of Pd, Pd-Ni, Pd-Sn and Pd-Ca catalysts



**Fig. 2** H$_2$-SCR performances over Pd-Sn catalysts with different Sn loading. **a** NO$_x$ conversion; **b** N$_2$ selectivity

## 3.3 $H_2$-TPR

The redox properties of Ni, Sn and Ca modified Pd catalysts were investigated by $H_2$-TPR and the profiles are shown in Fig. 4. For Pd alone, a small peak appears around 115 °C, which is due to the reduction of PdO [33]. It should be noted that $H_2$-TPR profiles of Pd-Ni, Pd-Sn and Pd-Ca are significantly different from that of Pd alone. For Pd-Ni catalyst, no $H_2$ consumption peak was observed below 300 °C, indicating that Pd mainly exists in the form of $Pd^0$, which is favorable for improving the $N_2$ selectivity [34] according to eq. (1). The small peak at 360 °C could be associated with the reduction peak of PdNi alloy [33]. In the case of Pd-Sn, a broad reduction peak centered at 190 °C can be observed. It could be attributed to the reduction of $Pd_3Sn_2$ and $Pd_3Sn$ alloy [35]. The reduction peak of tin oxide to metallic tin is absent [36], indicating that Sn is mainly present in the form of PdSn alloy. The $H_2$-TPR result of Pd-Sn is in accordance with XRD, both of which suggest the high dispersion of Pd and the existence
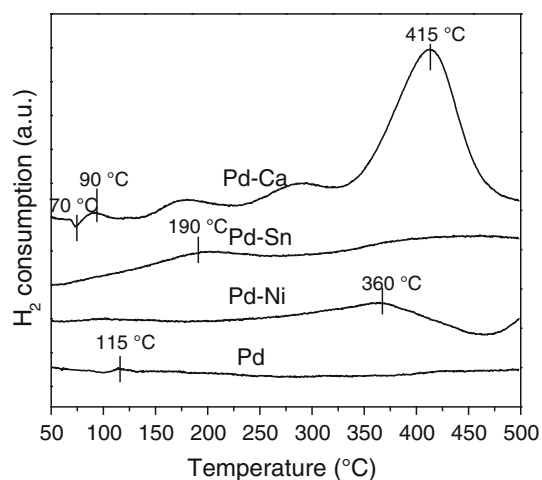
of strong interaction between Pd and Sn. Over Pd-Ca catalyst, the small negative reduction peak at 70 °C corresponds to the decomposition of β-palladium hydrides [37]. It is known that over the metallic Pd $H_2$ molecule will dissociate at room temperature, and the small dissociated hydrogen atom can enter the lattice of metallic Pd, forming β-palladium hydrides. On big crystallites of Pd palladium hydrides are more easily formed, while on the highly dispersed Pd the formation is considerably suppressed. Based on this, Pd over Pd-Ca catalyst is supposed to be present in the form of big crystallites with the poor dispersion, which is also confirmed by BET results. Furthermore, the relatively big peak around 90 °C ascribed to the reduction of PdO also reveals the same result. It is noted that there is one $H_2$ consumption peak around 415 °C, which could be attributed to the reduction of the surface capping oxygen of $TiO_2$ [38]. Different from Ni and Sn promoter, Ca is supposed to be present in the form of CaO over Pd-Ca catalyst. Chiarello et al. [39] reported that over $Pd/LaCoO_3$ catalyst the formation of PdCo alloy contributes to improving the $H_2$-SCR performance. Therefore, the promoting effect of Ni and Sn can be attributed to the formed alloy. Correlated to the $H_2$-SCR activity of Pd, Pd-Ni, Pd-Sn and Pd-Ca catalysts, it is concluded that both the dispersion of Pd and the redox property play significant roles on the catalytic performance for the $H_2$-SCR of $NO_x$.



**Fig. 4** $H_2$-TPR profiles of Pd, Pd-Ni, Pd-Sn and Pd-Ca catalysts

## 3.4 $NO_x$-TPD

$NO_x$-TPD has been carried out to investigate the $NO_x$ adsorption over the investigated catalysts. Figure 5 shows the $NO_x$-TPD profiles over the modified and unmodified catalysts. It can be seen that Pd-Ni and Pd-Sn catalysts exhibit the similar profiles, with a sharp peak at low temperature (<150 °C) and a broad one at high temperature (150–550 °C). Compared with Pd catalyst, the adsorption of $NO_x$ on Pd-Ni and Pd-Sn catalysts are remarkably increased. Therefore, these two catalysts are of higher $NO_x$
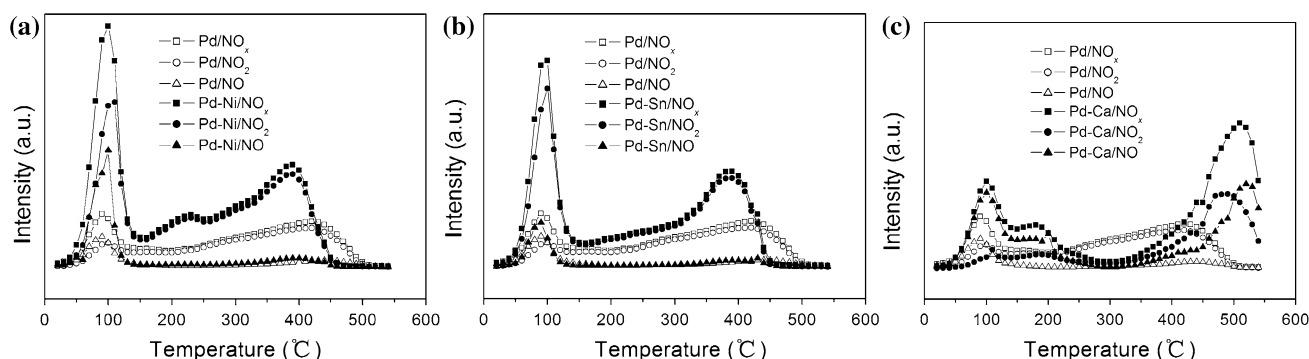


**Fig. 5** $NO_x$-TPD profiles over Pd-Ni and Pd (**a**), Pd-Sn and Pd (**b**), Pd-Ca and Pd (**c**) catalysts

adsorption capacity than Pd alone. The adsorption of $NO_x$ is important for the $H_2$-SCR to proceed. It should be noted that more $NO_2$ formed at low temperature over Pd-Sn catalyst than Pd-Ni catalyst. $NO_2$ is one key reaction intermediate in the $H_2$-SCR of $NO_x$ [40, 41]. The higher activity of Pd-Sn than Pd-Ni could be due to more $NO_2$ formed in the $H_2$-SCR reaction. In addition, excess of $NO_x$ adsorbed over the Pd-Ni catalyst leads to the occupation of active sites and thus limits active sites available for the adsorption and activation of $H_2$. This could be another reason for the lower activity of Pd-Ni than Pd-Sn. In the case of Pd-Ca catalyst, even less amount of $NO_2$ was adsorbed on it compared with the single Pd catalyst, implying that the adsorbed NO is hard to be oxidized into $NO_2$ and thus this catalyst showed poor catalytic performance for the $H_2$-SCR of $NO_x$.

## 4 Conclusions

Pd/TiO$_2$-Al$_2$O$_3$ catalysts were modified by Ni, Sn and Ca and their catalytic performance for the $H_2$-SCR of $NO_x$ was evaluated. It was found that the addition of Ni and Sn to Pd catalyst leads to the increased $NO_x$ conversion and $N_2$ selectivity above 200 °C. The promoting effect is more noticeable in the case of Sn addition and the optimum Sn loading is 2 %. The added Sn leads to the highly dispersed Pd, the formation of $Pd^0$ and the strong interaction between Sn and Pd. All of these contribute to the adsorption of NO and the oxidation of NO to $NO_2$, which was one key reaction intermediate in the $H_2$-SCR of $NO_x$. As a result, Pd-Sn catalyst showed higher catalytic performance than the Pd alone. In contrast, Pd-Ca catalyst showed poor $H_2$-SCR performance, which can be attributed to the increased average particle size and the decreased BET surface area after the addition of Ca.

## References

1. Wu P, Yu Q, Yan JJ et al (2010) Progress in selective catalytic reduction of $NO_x$ by hydrogen in excess oxygen. Chin J Catal 31:912–918
2. David B (2011) International private and public reinforcing dependencies for the innovation of automotive emission control systems in Japan and USA. Transport Res A 45:375–388
3. Bal RD, Dong SJ, Si HL et al (2008) Removal of NO from flue gas by aqueous chlorine-dioxide scrubbing solution in a lab-scale bubbling reactor. J Hazard Mater 150:649–655
4. Fredrik K, Kalle A, Kari E et al (2006) Toward improved catalytic low-temperature NO removal in diesel-powered vehicles. Acc Chem Res 39:273–282
5. Savva PG, Costas NC (2011) Hydrogen lean-DeNO$_x$ as an alternative to the ammonia and hydrocarbon selective catalytic reduction (SCR). Catal Rev Sci Eng 53:91–151
6. Shi XY, Yu YB, He H et al (2008) Combination of biodiesel–ethanol–diesel fuel blend and SCR catalyst assembly to reduce emissions from a heavy-duty diesel engine. J Environ Sci China 20:177–182
7. Yu YB, Zhao JJ, Yan Y et al (2013) A cyclic reaction pathway triggered by ammonia for the selective catalytic reduction of $NO_x$ by ethanol over Ag/Al$_2$O$_3$. Appl Catal B 136–137:103–111
8. Burch R, Coleman MD (1999) An investigation of the NO/H$_2$/O$_2$ reaction on noble metal catalysts at low temperature under lean-burn condition. Appl Catal B 23:115–121
9. Machida M, Ikeda S, Kurogi D et al (2001) Low temperature catalytic $NO_x$–$H_2$ reactions over Pt/TiO$_2$–ZrO$_2$ in an excess oxygen. Appl Catal B 35:107–116
10. Nanba T, Kohno C, Masukawa S et al (2003) Improvements in the $N_2$ selectivity of Pt catalysts in the NO–H$_2$–O$_2$ reaction at low temperatures. Appl Catal B 46:353–364
11. Machida M, Watanabe T (2004) Effect of Na-addition on catalytic activity of Pt-ZSM-5 for low-temperature NO–H$_2$–O$_2$ reactions. Appl Catal B 52:281–286
12. Costa NC, Angelos ME (2007) Mechanistic aspects of the $H_2$-SCR of NO on a novel Pt/MgO–CeO$_2$ catalyst. J Phys Chem C 111:3010–3020
13. Stefania F, Nunzio R, Debora F et al (2010) NO SCR reduction by hydrogen generated in on perovskite-type catalysts for automobile diesel exhaust gas treatment. Chem Eng Sci 65:120–127
14. Liu ZM, Li JH, Woo SI (2012) Recent advances in the selective catalytic reduction of $NO_x$ by hydrogen in the presence of oxygen. Energy Environ Sci 5:8799–8814
15. Hideaki H, Masaaki H (2012) A review of selective catalytic reduction of nitrogen oxides with hydrogen and carbon monoxide. Appl Catal A 421–422:1–13
16. Melanie L, Florian JPS, Michael B et al (2012) $NO_x$ reduction by $H_2$ on WO$_x$/ZrO-supported Pd catalysts under lean condition. Appl Catal B 117–118:275–282
17. Greenhalgh B, Charland JP, Stanciulescu M et al (2010) Pd-promoted catalysts for low temperature diesel engine DeNO$_x$. Catal Today 151:285–290
18. Yue BH, Zhou RX, Zheng XM et al (2008) Promotional effect of Ca on the Pd/Ce–Zr/Al$_2$O$_3$ catalyst for low-temperature catalytic combustion of methane. Fuel Process Technol 89:728–735
19. Wang G, Meng M, Zha YQ et al (2010) High-temperature close coupled catalysts Pd/Ce–Zr–M/Al$_2$O$_3$ (M=Y, Ca or Ba) used for the total oxidation of propane. Fuel 89:244–251
20. Liu ZM, Li JH, Hao JM (2010) Selective catalytic reduction of $NO_x$ with propene over SnO$_2$/Al$_2$O$_3$ catalyst. Chem Eng J 165:420–425
21. Li JH, Hao JM, Fu LX et al (2004) The activity and characterization of sol–gel Sn/Al$_2$O$_3$ catalyst for selective catalytic reduction of $NO_x$ in the presence of oxygen. Catal Today 90:215–221
22. Corro G, Fierro JLG, Montiel R et al (2003) A highly sulfur resistant Pt-Sn–/Al$_2$O$_3$ catalyst for C$_3$H$_8$–NO–O$_2$ reaction under lean conditions. Appl Catal B 46:307–317
23. Li DC, Wang LJ, Zhang P et al (2013) HI decomposition over active carbon supported binary Ni–Pd catalysts prepared by electroless plating. Catal Commun 37:32–35
24. Amin RS, Hameed RMA, El-Khatib KM (2014) Microwave heated synthesis of carbon supported Pd, Ni and Pd–Ni nanoparticles for methanol oxidation in KOH solution. Appl Catal B 148–149:557–567

25. Li LD, Zhang FX, Guan NJ et al (2008) NO selective reduction by hydrogen on potassium titanate supported palladium catalyst. Catal Commun 9:1827–1832

26. Li J, Wu GJ, Guan NJ et al (2012) NO selective reduction by hydrogen over bimetallic Pd–Ir/TiO$_2$ catalyst. Catal Commun 24:38–43

27. Chen Y, He J, Ma YG et al (2007) Investigation of NO$_x$ storage and sulfur resistance of Pd/TiO$_2$/γ-Al$_2$O$_3$. J Mol Catal 21:427–432 (in Chinese)

28. Xia SM, Xu CS, Zhang ML et al (2009) Preparation and photocatalytic property of TiO$_2$/SiO$_2$/NiFe$_2$O$_4$ magnetic nano-particles. Chem Res Appl 04:455–458 (in Chinese)

29. Norman M, Rachael C, James MK et al (2004) Exploiting the synergy of titania and alumina in lean NO$_x$ reduction in situ ammonia generation during the Pd/TiO$_2$–Al$_2$O$_3$ catalyzed H$_2$/CO/NO/O$_2$ reaction. J Catal 221:20–31

30. Arunkumar S, Pratyay B, Satyanarayana L et al (2013) Hierarchical SnO/SnO$_2$ nanocomposites: formation of in situ p–n junctions and enhanced H$_2$ sensing. Sens Actuators B 185:265–273

31. Anthony G, Károly L, Florence E (2005) Effect of the support on tin distribution in Pd–Sn/Al$_2$O$_3$ and Pd–Sn/SiO$_2$ catalysts for application in water denitration. Appl Catal B 59:57–69

32. Zhao J, Xu XL, Li XN et al (2014) Promotion of Sn on the Pd/AC catalyst for the selective hydrogenation of cinnamaldehyde. Catal Commun 43:102–106

33. Tanksale A, Beltramini JN, Dumesic JA et al (2008) Effect of Pt and Pd promoter on Ni supported catalysts—a TPR/TPO/TPD and microcalorimetry study. J Catal 258:366–377

34. Nan BCK, Masukawa S, Uchisawa J et al (2003) Improvements in the N$_2$ selectivity of Pt catalysts in the NO–H$_2$–O$_2$ reaction at low temperature. Appl Catal B 46:353–364

35. Devadas A, Vasudevan S, Epron F (2011) Nitrate reduction in water: influence of the addition of a second metal on the performances of the Pd/CeO$_2$ catalyst. J Hazard Mater 185:1412–1417

36. Adagneves OC, Luciana SF, Fabio BP et al (2012) Microkinetic modeling of the hydrogenation of nitrate in water on Pd–Sn/Al$_2$O$_3$ catalyst. Appl Catal A 445–446:26–34

37. Wang G, You R, Meng M (2013) An optimized highly active and thermo-stable oxidation catalyst Pd/Ce–Zr–Y/Al$_2$O$_3$ calcined at superhigh temperature and used for C$_3$H$_8$ total oxidation. Fuel 103:799–804

38. Zhang CB, He H, Tanaka K (2006) Catalytic performance and mechanism of a Pt/TiO$_2$ catalyst for the oxidation of formaldehyde at room temperature. Appl Catal B 65:37–43

39. Chiarello GL, Ferri D, Grunwaldt JD et al (2007) Flame-synthesized LaCoO$_3$-supported Pd: 2. Catalytic behavior in the reduction of NO by H$_2$ under lean conditions. J Catal 252:137–147

40. Hu YH, Griffiths K, Norton PR (2009) Surface science studies of selective catalytic reduction of NO: progress in the last ten years. Surf Sci 603:1740–1750

41. Petros GS, Angelos ME (2008) The influence of reaction temperature on the chemical structure and surface concentration of active NO$_x$ in H$_2$-SCR over Pt/MgO–CeO$_2$: SSITKA-DRIFTS and transient mass spectrometry studies. J Catal 257:324–333